

Spectroscopic Constraints on the Stellar Population of Elliptical Galaxies in the Coma Cluster

B. Mobasher^{1,2} and P. A. James³

¹ *Astrophysics Group, Blackett Laboratory, Imperial College, Prince Consort Rd, London SW7 2BZ, UK*

² *Space Telescope Science Institute, 3700 San Martin Drive, Baltimore, MD 21218, USA*

³ *Astrophysics Research Institute, Liverpool John Moores University, Egerton Wharf, Birkenhead, CH41 1LD, UK*

26 October 2018

ABSTRACT

Near-IR spectra for a sample of 31 elliptical galaxies in the Coma cluster are obtained. The galaxies are selected to be ellipticals (no lenticulars), with a large spatial distribution, covering both the core and outskirt of the cluster (ie. corresponding to regions with large density contrasts). CO_{sp} (2.3 μ m) absorption indices], measuring the contribution from intermediate-age red giant and supergiant stars to the near-IR light of the ellipticals, are then estimated.

It is found that the strength of CO_{sp} features in elliptical galaxies increases from the core ($r < 0.2^\circ$) to the outskirts ($r > 0.2^\circ$) of the Coma cluster. Using the Mg₂ strengths, it is shown that the observed effect is not due to metallicity and is mostly caused by the presence of a younger population (giant and supergiant stars) in ellipticals in outskirts (low density region) of the cluster.

Using the CO_{sp} features, the origin of the scatter on the near-IR Fundamental Plane (relation between the effective diameter, effective surface brightness and velocity dispersion) of elliptical galaxies is studied. Correcting this relation for contributions from the red giant and supergiant stars, the *rms* scatter reduces from 0.077dex to 0.073dex. Although measurable, the contribution from these intermediate-age stars to the scatter on the near-IR Fundamental Plane of ellipticals is only marginal.

A relation is found between the CO_{sp} and $V - K$ colours of ellipticals, corresponding to a slope of 0.036 ± 0.016 , significantly shallower than that from the Mg₂ – ($V - K$) relation. This is studied using stellar synthesis models.

Key words: galaxies: clusters - galaxies: elliptical - galaxies: fundamental parameters - galaxies: stellar content- infrared: galaxies

1 INTRODUCTION

There is growing evidence that early-type galaxies located in small groups and in the field may possess an intermediate-age stellar component ($\sim 1 - 5$ Gyrs), in addition to the old stellar population characteristic of their cluster counterparts (Bothun & Gregg 1990; Caldwell et al. 1996). For example, using the strength of optical spectral lines, the presence of a substantial population of intermediate-age stars is confirmed in elliptical galaxies in low density environments, an effect which is much reduced in ellipticals in denser regions (Bower et al 1990; Rose et al 1994). This is further supported by spectroscopic ($H\beta$) and photometric (UV-optical colours) observations of field ellipticals, showing evidence for star formation in these galaxies within the last 3 – 5 Gyrs (Schweizer & Seitzer 1992; Gonzalez 1993).

This systematic difference in age poses serious problems in using relations established for cluster ellipticals to study field galaxies. For example, the Fundamental Plane (FP) relation between the velocity dispersion, effective surface brightness and effective radius of ellipticals, used to measure the peculiar velocity field and to study the evolution and formation of galaxies, is often zero-pointed using cluster samples. Any difference between the cluster and field populations will lead to spurious results. The effect of this intermediate-age stellar population on the FP of ellipticals in low density environments is investigated by Guzmán et al (1994).

Recently, an attempt has been made to reduce the contribution from this young population on the FP of ellipticals by extending this relation to near-IR ($2.2 \mu m$) wavelengths (Pahre et al 1998; Mobasher et al 1999). The near-IR FP is expected to be less affected by differences in age, metallicity and stellar population among the ellipticals, compared to its optical counterpart. Therefore, the relatively large *rms* scatter found for the near-IR relation (0.076 dex and 0.074 dex for the infrared and optical relations respectively) is surprising. This is either due to contributions to their near-IR light from the red giant and supergiant stars, or is caused by differences in matter distribution and the internal dynamics (i.e. orbital anisotropy or rotation) among the ellipticals. Understanding the origin of this scatter is essential in constraining models of formation and evolution of elliptical galaxies.

A good indicator of the presence of an intermediate-age stellar population in elliptical galaxies is the strength of their spectroscopic near-IR CO ($2.3\ \mu\text{m}$) absorption feature, since this is mainly produced in the atmosphere of giant and supergiant stars. Also, unlike Mg_2 line indices, these are relatively insensitive to the on-going star formation (ie. formation of main sequence stars prior to the formation of the giant and supergiant populations) and extinction by dust. In a recent study, the value of near-IR CO bandheads in constraining stellar population of elliptical galaxies is explored (Mobasher & James 1997; James & Mobasher 1999). Measuring CO strengths for a small and heterogeneous sample of cluster and field ellipticals, the presence of a younger component in at least some field ellipticals was confirmed. Here, we extend this study to ellipticals at the core and outskirts of the Coma cluster. This provides a homogeneous sample for studying the stellar population of ellipticals in regions with large density contrasts. By choosing the ellipticals at the core and outskirt of a single cluster, we aim to minimise the contribution due to chemical evolution in galaxies as a function of environment, with the *only* difference being the local density.

Section 2 presents the spectroscopic observations and data reduction. A discussion of the physical significance of the strength of near-IR CO features is given in section 3. This is followed in section 4 by a study of the radial dependence of CO strengths in the Coma ellipticals. Section 5 explores the source of the scatter in the near-IR FP of ellipticals. The relation between the strength of CO features and other photometric parameters in ellipticals is studied in section 6. The conclusions are summarised in section 7.

2 SAMPLE SELECTION, OBSERVATIONS AND DATA REDUCTION

The galaxies for this study are selected to be ellipticals (i.e. no lenticulars), confirmed members of the Coma cluster and have a wide enough spatial distribution to cover both the core and outskirts of the cluster (i.e. regions with large density contrast). Other spectroscopic (velocity dispersion, Mg_2 line strengths) and photometric (optical and near-IR luminosities) data are available for all the galaxies in the sample.

The observations were carried out using the United Kingdom Infrared Telescope (UKIRT) during the 4 nights of 21–24 February 1999. The instrument used was the long-slit near-IR spectrometer CGS4, with the $40\ \text{line mm}^{-1}$ grating and the long-focal-length (300 mm) camera. The 4-pixel-wide slit was chosen, corresponding to a projected width on the sky of 2.4 arcsec. Working in 1st order at a central wavelength of $2.2\ \mu\text{m}$, this gave coverage of the

entire K window. The CO absorption feature, required for this study, extends from 2.293 μm (rest frame) into the K-band atmospheric cut-off. The principal uncertainty in determining the absorption depth comes from estimating the level and slope of the continuum shortward of this absorption which requires wavelength coverage down to at least 2.2 μm and preferably shorter. There are many regions of the continuum free from lines even at this relatively low resolution. The effective resolution, including the degradation caused by the wide slit, is about 230.

For each observation, the galaxy was centred on the slit by maximising the IR signal, using an automatic peak-up facility. Total on-chip integration times of 12 minutes were used for the brightest and most centrally concentrated ellipticals while an integration time of 24 minutes was more typically required. During this time, the galaxy was slid up and down the slit at one minute intervals by 22 arcsec, giving two offset spectra which were subtracted to remove most of the sky emission. Moreover, the array was moved by 1 pixel between integrations to enable bad pixel replacement in the final spectra. Stars of spectral types A0–A6, suitable for monitoring telluric absorption, were observed in the same way before and after each galaxy, with airmasses matching those of the galaxy observations as closely as possible. Flat fields and argon arc spectra were taken using the CGS4 calibration lamps. A total of 31 elliptical galaxies in the core and outskirts of the Coma cluster were observed.

The data reduction was performed using the FIGARO package in the STARLINK environment. The spectra were flatfielded and a polynomial was fitted to estimate and remove the sky background. These spectra were then shifted to the rest frame of the galaxy, using their redshifts. The atmospheric transmissions were corrected by dividing the spectra with the spectrum of the standard star observed closely in time to the galaxy, and at a similar airmass. The resulting spectra was converted into a normalised, rectified spectrum by fitting a power-law to featureless sections of the continuum and dividing the whole spectrum by this power-law, extrapolated over the full wavelength range.

To measure the depth of the CO absorption feature, the same procedure outlined in James and Mobasher (1999) is used. The restframe, rectified spectra were rebinned to a common wavelength range and number of pixels, to avoid rounding errors in the effective wavelength range sampled by a given number of pixels. Two methods were then used to define the CO strength for each spectrum. The first is the spectroscopic CO index (Doyon et al. 1994), CO_{sp} , which is the mean level of the rectified spectrum, between wavelength limits of 2.31 μm and 2.4 μm , expressed as a magnitude difference, relative to the continuum level. The second

measurement was the CO equivalent width (Puxley, Doyon & Ward 1998), CO_{EW} , which quantifies the depth of the CO absorption between $2.293\ \mu\text{m}$ and $2.32\ \mu\text{m}$. Both CO_{sp} and CO_{EW} are defined such that a deeper absorption corresponds to a larger number. CO_{sp} has the advantage that the fractional Poisson errors are decreased by averaging the absorption over a larger wavelength range, whereas CO_{EW} is claimed to be more sensitive to stellar population variations, and is less subject to errors in the power-law fitting. Also, CO_{EW} can be used for higher redshift galaxies, due to the shorter wavelength range, although that is not a consideration for the present study.

There are three principal and quantifiable sources of error in the measured CO_{sp} values here. The first is due to pixel-to-pixel noise in the reduced spectra, as calculated from the standard deviation in the fitted continuum points, assuming that the noise level remains constant through the CO absorption. This gives an error on both the continuum level and the mean level in the CO_{sp} absorption, which were added in quadrature. The second error component comes from the formal error provided by the continuum fitting procedure. This could leave a residual tilt or curvature in the spectrum. The formal error was used to quantify this contribution. The final component is an estimate of the error induced by redshift and wavelength calibration uncertainties. All three errors were of similar sizes, and when added in quadrature give a typical uncertainty in CO_{sp} of ± 0.012 mag. Furthermore, we repeated one galaxy (NGC 2832) on separate nights. The completely independent reductions of the two observations gave CO_{sp} indices corresponding to 0.257 mag. and 0.263 mag. This is consistent with the random components of the error calculation above, and well within our total error estimate.

The strength of CO absorption features and their corresponding equivalent widths for the Coma ellipticals observed in this study are presented in Table 1. Column 2 lists the radial distance (in degrees) from the core of the Coma cluster. Columns 3-6 give, respectively, the total near-IR magnitudes (K_{tot}), velocity dispersions ($\log(\sigma)$), optical-IR colours ($V - K$) and spectroscopic Mg₂ measurements, all taken directly from Table 1 in Mobasher et al (1999). Finally, estimates of the CO_{sp} and CO_{EW} are given in columns 7 and 8 respectively.

To allow the comparison between the CO_{sp} features from the present sample and those for higher redshift ellipticals (for which only CO_{EW} is measurable), the relation between the CO strength of absorption feature and the CO equivalent width for individual galaxies is presented in Figure 1. A least squares fit to this relation gives

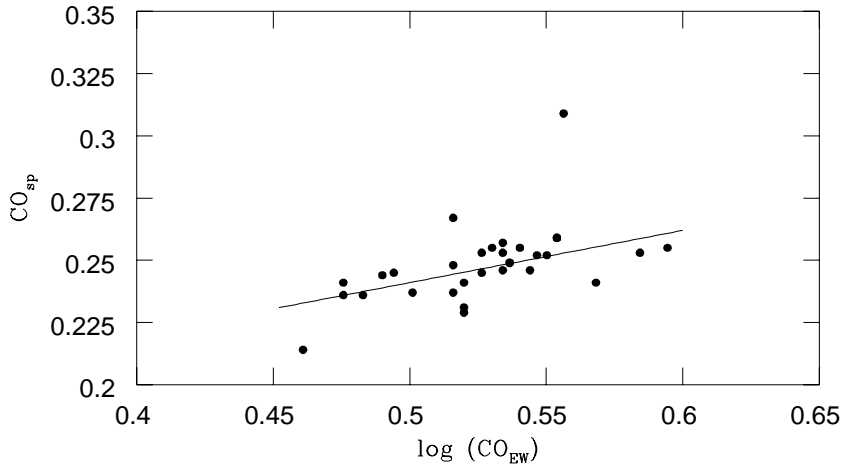


Figure 1. The CO_{sp} – CO_{EW} relation for the sample of elliptical galaxies in Table 1. The linear least squares fit to the data is also shown. The galaxy N4971 is $> 3\sigma$ deviant from the mean relation and is not included in the fit.

$$\text{CO}_{sp} = (0.210 \pm 0.005) \log (\text{CO}_{EW}) + (0.136 \pm 0.005)$$

with $rms = 0.008$. The deviant point in Figure 1 is N4971, which is excluded from the fit. For the analysis in the following sections, the CO_{sp} strengths are used (in magnitude units). For nearby galaxies, where the CO_{sp} is not heavily contaminated by atmospheric lines, this is a reasonable procedure. The subsequent results in this paper do not depend on whether the CO_{sp} or CO_{EW} are used.

Table 1. The photometric and spectroscopic parameters for elliptical galaxies in the Coma cluster

Name	r	K_{tot}	$log(\sigma)$	$V - K$	Mg2	CO_{EW}	CO_{sp}
RB45	0.040	11.91	2.133	3.10	0.280	3.31	0.231
N4886	0.050	10.86	2.209	2.95	0.254	3.70	0.241
RB43	0.056	12.19	2.230	3.01	0.262	2.99	0.236
N4889	0.060	8.20	2.595	3.32	0.348	3.55	0.252
N4874	0.060	8.55	2.398	3.26	0.323	3.31	0.229
N4876	0.062	10.89	2.267	3.19	0.242	2.89	0.214
IC4011	0.064	11.78	2.061	3.04	0.279	3.17	0.237
N4872	0.069	11.30	2.329	3.09	0.300	3.50	0.246
IC4021	0.112	11.58	2.205	3.23	0.299	3.09	0.244
N4869	0.119	10.27	2.303	3.23	0.315	3.93	0.255
IC4012	0.125	11.40	2.258	3.30	0.292	3.42	0.253
N4867	0.135	11.12	2.352	3.17	0.307	2.99	0.241
N4864	0.144	10.15	2.289	—	0.286	3.42	0.257
N4906	0.181	10.89	2.228	3.17	0.288	3.42	0.246
D204	0.404	11.84	2.114	3.05	0.268	3.04	0.236
D160-100	0.441	11.47	2.269	3.20	0.285	3.28	0.267
N4926	0.565	9.80	2.420	3.32	0.324	3.47	0.255
N4841A	0.723	9.53	2.414	3.24	0.320	3.58	0.259
D140	0.745	11.42	2.232	3.13	0.297	3.84	0.253
D160-27	0.768	11.30	2.235	3.14	0.282	3.31	0.241
N4816	0.839	9.95	2.330	3.24	0.310	3.58	0.259
IC4133	0.879	11.18	2.233	3.14	0.289	3.44	0.249
N4807	1.067	10.28	2.310	3.17	0.285	3.36	0.245
IC843	1.221	10.02	2.389	3.51	0.303	3.52	0.252
N4789	1.525	9.30	2.416	3.25	0.304	3.44	0.249
N4971	1.656	10.57	2.250	3.28	0.291	3.60	0.309
D159-83	2.500	10.23	2.306	3.38	0.275	3.39	0.255
D160-159	2.790	10.66	2.358	3.24	0.280	3.28	0.237
N4673	3.294	9.68	2.345	3.18	0.270	3.36	0.253
D159-43	4.545	10.60	2.399	3.33	0.338	3.28	0.248
D159-41	4.750	11.11	2.277	3.23	0.324	3.12	0.245

3 WHAT DO NEAR-IR CO INDICES MEASURE IN ELLIPTICAL GALAXIES ?

The CO band at $2.3\mu m$, lies longward of $2.29\mu m$ and constitutes the strongest absorption feature in the K spectrum. Beyond about $2.5\mu m$, the near-infrared spectrum is contaminated by the atmospheric OH lines, producing spurious absorption features and low atmospheric transmission. The $2.3\mu m$ CO absorption feature is present in the atmosphere of red giant (including Asymptotic Giant Branch- AGB) and supergiant stars. Its depth increases with decreasing stellar temperature, increasing stellar luminosity (Kleinman & Hall 1986), and increasing metallicity (Aaronson et al 1978). This implies that red giant and supergiant stars have deeper CO absorption features than dwarf stars. Moreover, supergiants are expected to have stronger CO features than giant stars of the same temperature (this is because the former have a higher microturbulent velocity, implying that the CO absorption band is made of many saturated lines, leading to reduced dependence of metallicity on the CO strength). For example, Doyon et al (1994) found that the strength of the CO band associated with a

young stellar population reaches a maximum between 15 and 40 Myrs and a CO_{sp} index of ~ 0.28 mag. This is ~ 0.1 mag higher than that observed for normal galaxies and is due to a contribution from red supergiants.

Since the CO strengths provide a diagnostic for identifying the young to intermediate age AGB and supergiant population in galaxies, and because of its relative insensitivity to non-stellar radiation and dust reddening, these features have been widely used to identify stellar populations in dusty infrared luminous galaxies (i.e. starbursts)- (Goldader et al 1997; Doyon et al 1994; Ridgway et al 1994). However, such studies are complicated by the fact that the CO strength also depends to some extent on the metallicity, in spite of the effects noted in the previous paragraph. This effect has been studied by Frogel, Cohen & Persson (1983), using globular clusters with measured metallicities and photometric CO indices. Using this calibration and the transformation between photometric and spectroscopic CO features, Doyon et al (1994) find $\Delta(CO_{sp}) = 0.11\Delta[Fe/H]$, where $[Fe/H]$ is the logarithm of metal abundance relative to the Sun.

To use the CO strengths to study evolutionary properties of elliptical galaxies, it is therefore important to separate the relative contributions from metallicity and stellar population. There is currently no population synthesis models for composite stellar systems with satisfactory treatment of the intermediate age AGB and red supergiants and hence, near-IR CO features. Using the sample of Coma ellipticals in Table 1, we find a relation between their CO_{sp} and Mg_2 strengths (Figure 2). A linear fit to the 30 galaxies (excluding N4971) with available CO_{sp} and Mg_2 gives

$$CO_{sp} = (0.189 \pm 0.073)Mg_2 + (0.191 \pm 0.003)$$

with $rms = 0.01$. Assuming Mg_2 to be a measure of metallicity, the trend in Figure 2 demonstrates changes in CO indices due to metallicity, while the scatter in this diagram, at a given Mg_2 , indicates variations in CO indices due to contributions from AGB and supergiant stars to the near-IR light of ellipticals (this also includes measurement errors in CO indices). The slope here is steeper than 0.11 found by Doyon et al. (1994) which was estimated from the globular clusters, with most of them having sub-solar metallicities, requiring extrapolation beyond solar metallicity. Moreover, the Mg_2 indices for elliptical galaxies are also likely to be affected by the young population (i.e. residual star formation). Nevertheless, we use the relation in Figure 2 in subsequent sections to explore changes in

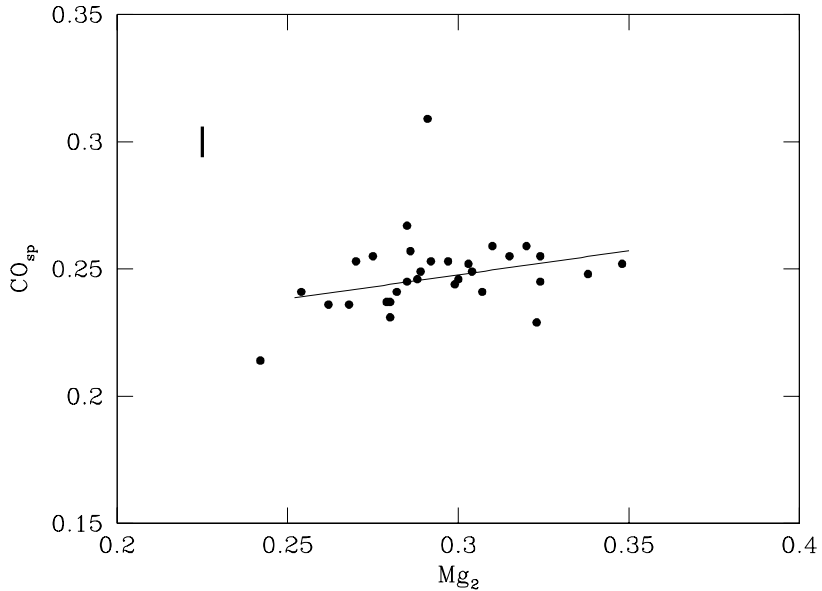


Figure 2. The CO_{sp} – Mg_2 relation for elliptical galaxies in the Coma cluster (Table 1). The linear least squares fit, excluding the deviant point (N4971), is also shown. The errorbar shows the uncertainty in CO_{sp} measurement for individual galaxies.

CO_{sp} strengths due to age and metallicity and to separate these effects from that due to contributions from the giant and supergiant stars.

4 SPECTROSCOPIC EVOLUTION OF ELLIPTICALS AS A FUNCTION OF ENVIRONMENT

The homogeneity of the present sample, combined with its spatial coverage, allows a study of the spectroscopic properties of ellipticals with radial distance (i.e. local density) from the core of the Coma cluster. The CO_{sp} histograms for elliptical galaxies at the core ($r < 0.2^\circ$) and outskirt ($r > 0.2^\circ$) of the Coma cluster are compared in Figure 3a, with their mean $\langle \text{CO}_{sp} \rangle$ values listed in Table 2. This shows that, on average, the ellipticals in the outskirts of the Coma cluster have a stronger CO_{sp} feature compared to those at the core. This is a $\sim 3\sigma$ effect, with $< 1\%$ chance of them belonging to the same parent population. Furthermore, considering a standard deviation of 0.012 mag. in the estimated CO_{sp} values for individual galaxies, the observational errors corresponding to mean CO_{sp} at the core (17 galaxies) and outskirt (14 galaxies) of the Coma cluster correspond to 0.0029 mag. and 0.0032 mag. respectively. These estimates are fully consistent with the errors quoted in Table 2. However, they imply that the bulk of the scatter is due to measurement errors.

For the same galaxies, distribution of the Mg_2 indices are also compared in Figure 3b with the mean $\langle \text{Mg}_2 \rangle$ values listed in Table 2. There are no significant changes in $\langle \text{Mg}_2 \rangle$

Table 2. Mean CO_{sp} and Mg_2 estimates for ellipticals at the core and outskirt of the Coma cluster and a sample of $z = 0.07$ clusters.

	$r < 0.2^\circ$	$r > 0.2^\circ$	Total
Coma			
$\langle \text{CO}_{sp} \rangle$	0.241 ± 0.003	0.254 ± 0.004	0.248 ± 0.005
$\langle \text{Mg}_2 \rangle$	0.291 ± 0.007	0.297 ± 0.005	0.294 ± 0.009
Pisces/A2199/A2634			
$\langle \text{CO}_{sp} \rangle$		0.244 ± 0.004	

strengths with radial distance from the core of the Coma. This implies that the observed difference in CO_{sp} strengths is not likely to be due to metallicity and is mainly caused by changes in contributions from the intermediate age AGB and supergiant population among the ellipticals at different distances from the cluster core.

The conclusion is that the ellipticals at low density regions of the Coma (ie. cluster outskirts) have a population of AGB and/or supergiant stars, not present in ellipticals at the denser (core) region, indicating that the galaxies in the outer parts of the Coma cluster are relatively younger than those at the core.

The variation in the CO_{sp} with the radial distance from the cluster core, shown in figure 4 The average scatter in the CO_{sp} , at a given radius, is 0.004 mag (corresponding to the scatter in the zero-point in the above relation), which is significantly less than the variation in CO_{sp} strength across the cluster, listed in Table 2. This confirms again the radial dependence of the CO_{sp} features for ellipticals in the Coma cluster.

To further study the environmental dependence of the stellar population in elliptical galaxies, the $\langle \text{CO}_{sp} \rangle$ values of 30 ellipticals in the Pisces, A2199 and A2634 clusters at $z = 0.07$ (James and Mobasher 1999), are compared to those in the Coma in figure 3c and Table 2. The $\langle \text{CO}_{sp} \rangle$ values for ellipticals in $z = 0.07$ clusters agree well with those at the core of the Coma cluster, indicating that they mostly consist of old population, unlike the galaxies in less dense environments, although the statistical significant of this result is rather marginal.

Since the present sample consists of elliptical galaxies (ie. no lenticulars), the observed trend is not likely to be due to a dramatic change in the galaxy population (eg. transition from SOs to ellipticals) with radial distance from the center of the cluster. However, it is more probable that the ellipticals in the outer parts of the Coma cluster are undergoing final stages of evolution before they stop star formation activity, while falling into the core of the

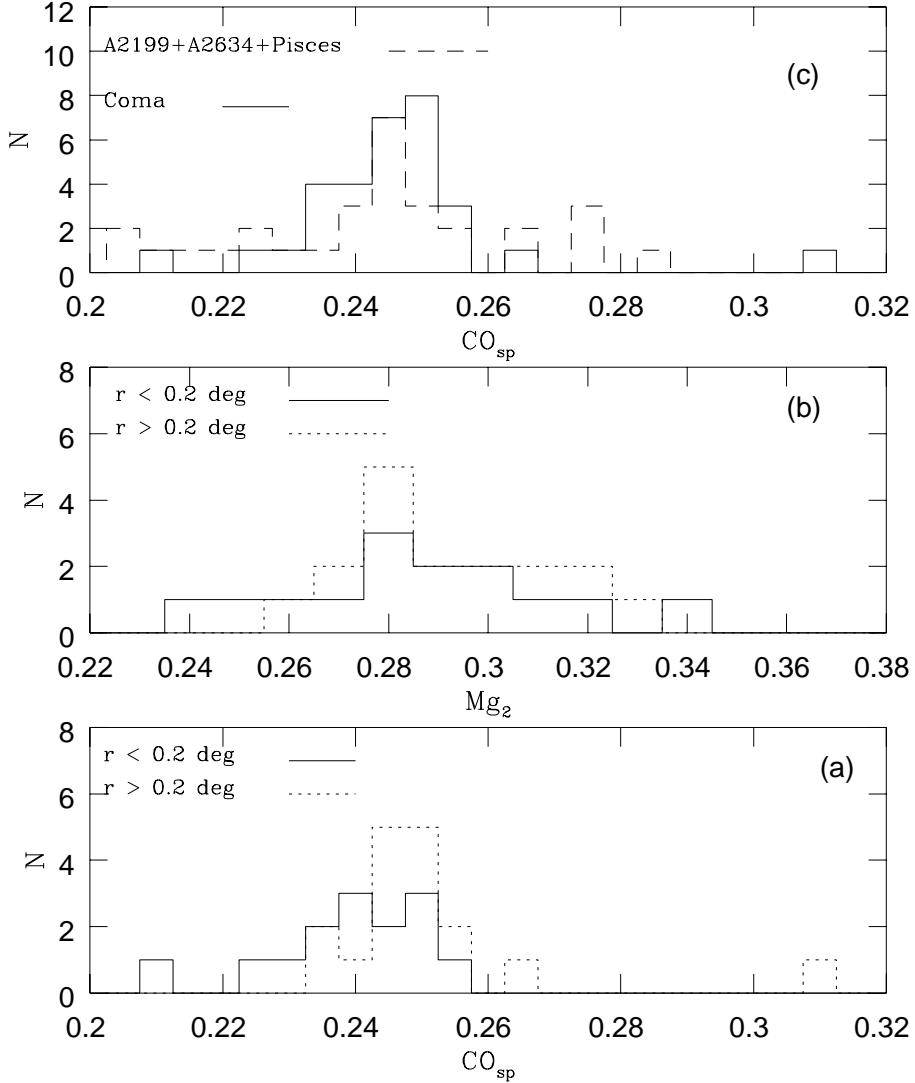


Figure 3. (a). Distribution of CO_{sp} for ellipticals at the core (solid line) and outskirts (dotted line) of the Coma cluster. (b). The same as 3a for Mg_2 indices. (c). Comparison between the CO_{sp} distribution for elliptical galaxies in the Coma (both core and outskirts)-(solid line) and the sample of ellipticals in A2199, A2634 and Pisces clusters at $z \sim 0.07$, taken from James & Mobasher (1999)-(dashed line).

cluster. Indeed, recent observations at the peripheries of high-redshift clusters ($0.2 < z < 1$), show a remarkable radial gradient in the distribution of colour, Balmer absorption lines and equivalent widths (Abraham et al 1996). Particularly striking is the gradient in the $H\delta$ strong systems, usually classed as “post-starburst” galaxies whose strong Balmer lines result from a sharp truncation in their rate of star formation. Moreover, observations of distant clusters have shown transitions of SO population to ellipticals towards the core of the clusters (Dressler et al 1998). Also, recent spectroscopic study of early-type galaxies in

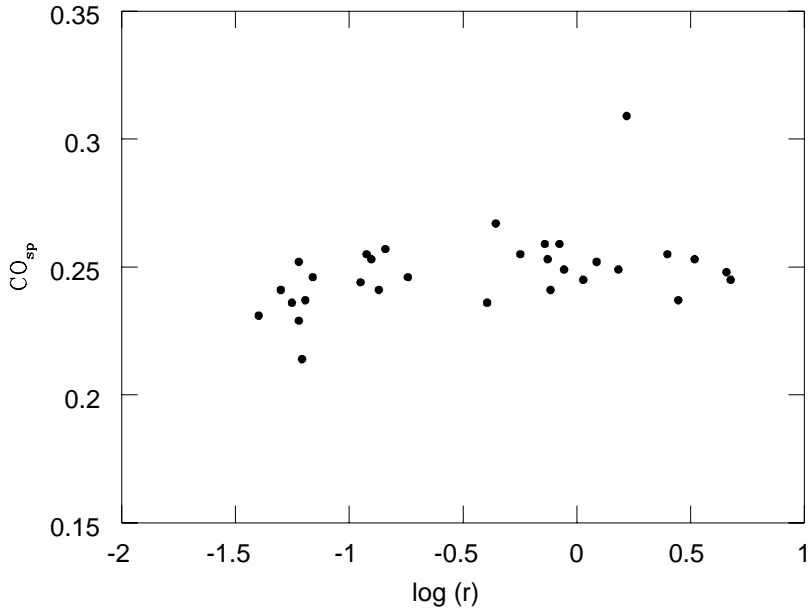


Figure 4. Changes of CO_{sp} with radial distance to ellipticals from the center of the Coma cluster.

the nearby Fornax cluster has revealed that the SOs have a relatively younger age than the ellipticals (Kuntschner & Davies 1998). Therefore, it is possible that the ellipticals, observed in the periphery of the Coma cluster, are local counterparts of the “post-starburst” (E+A) population or SO galaxies (undergoing latest stages of their evolution) observed at higher redshifts.

5 SOURCES OF SCATTER IN THE NEAR-INFRARED FUNDAMENTAL PLANE OF ELLIPTICALS

By extending the FP of elliptical galaxies to near-IR wavelengths, it is expected to minimise contributions from the young population and metallicity in this relation and hence, reduce the observed scatter (Pahre et al 1998; Mobasher et al 1999). However, it has been discovered that the observed scatter is not significantly reduced in the near-IR FP compared to its optical counterpart. A likely explanation is the relative contributions from the intermediate age AGB and red supergiant stars to the near-IR light of ellipticals (Mobasher et al 1999). This is explored in the present section, using the CO_{sp} strengths to measure the contribution from these stars.

Using the sample of 31 elliptical galaxies in the Coma cluster (Mobasher et al 1999), for which CO_{sp} measurements are available from the present study, a three parameter plane fit

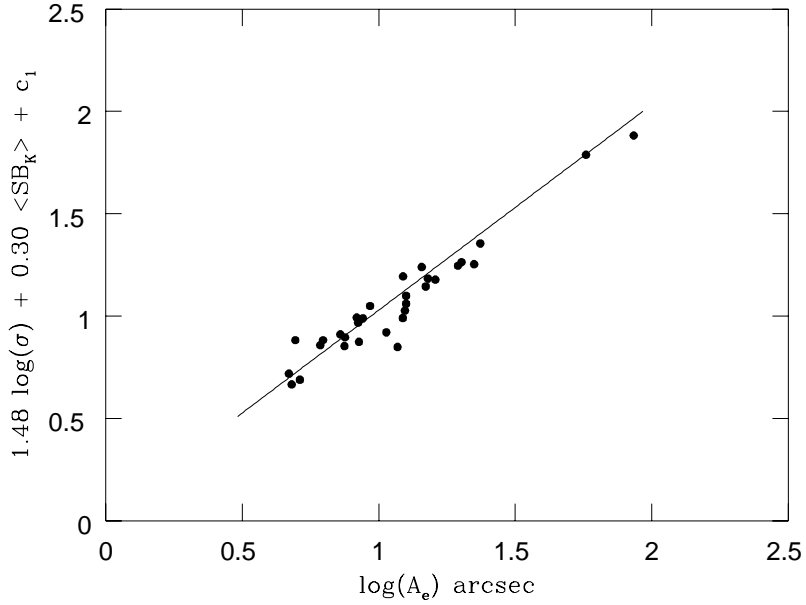


Figure 5. Near-IR FP of elliptical galaxies in the Coma cluster, using 31 galaxies listed in Table 1. The photometric data are taken from Mobasher et al (1999). The line is a three parameter plane fit to the data.

was carried out to the K-band effective surface brightness ($\langle SB_K \rangle_e$), effective diameter (A_e) and velocity dispersion (σ). This gives

$$\log A_e = 1.48 \log(\sigma) + 0.30 \langle SB_K \rangle_e - 7.24$$

with an *rms* scatter (in $\log A_e$) of 0.077 dex. An edge-on view of near-IR FP is shown in Figure 5.

The residuals from the the mean FP at a given $\log(A_e)$ —($\Delta(FP) = 1.48 \log(\sigma) + 0.30 \langle SB_K \rangle_e - 7.24 - \log A_e$), are estimated for individual galaxies and are found to be correlated with their CO_{sp} (Figure 6a). A least squares fit to this relation gives $\Delta(FP) = -0.858 CO_{sp} + 0.242$ with 98% likelihood of this being a true relation. This trend is also confirmed using CO_{EW} values for the Coma ellipticals from Table 1 (Figure 6b). However, no significant correlation is found between $\Delta(FP)$ and Mg_2 strengths (Figure 6c). The presence of a relation between $\Delta(FP)$ and CO_{sp} implies that the observed scatter on the near-IR FP of Coma ellipticals (Figure 5) is, at least partly, due to changes in the contribution from the giant and supergiant populations and is not a metallicity effect, as revealed from the absence of a relation between $\Delta(FP)$ and Mg_2 . This is consistent with the results from the previous section in which ellipticals in the Coma cluster were found to have different stellar populations, depending on their position (local density) in the cluster. Using the

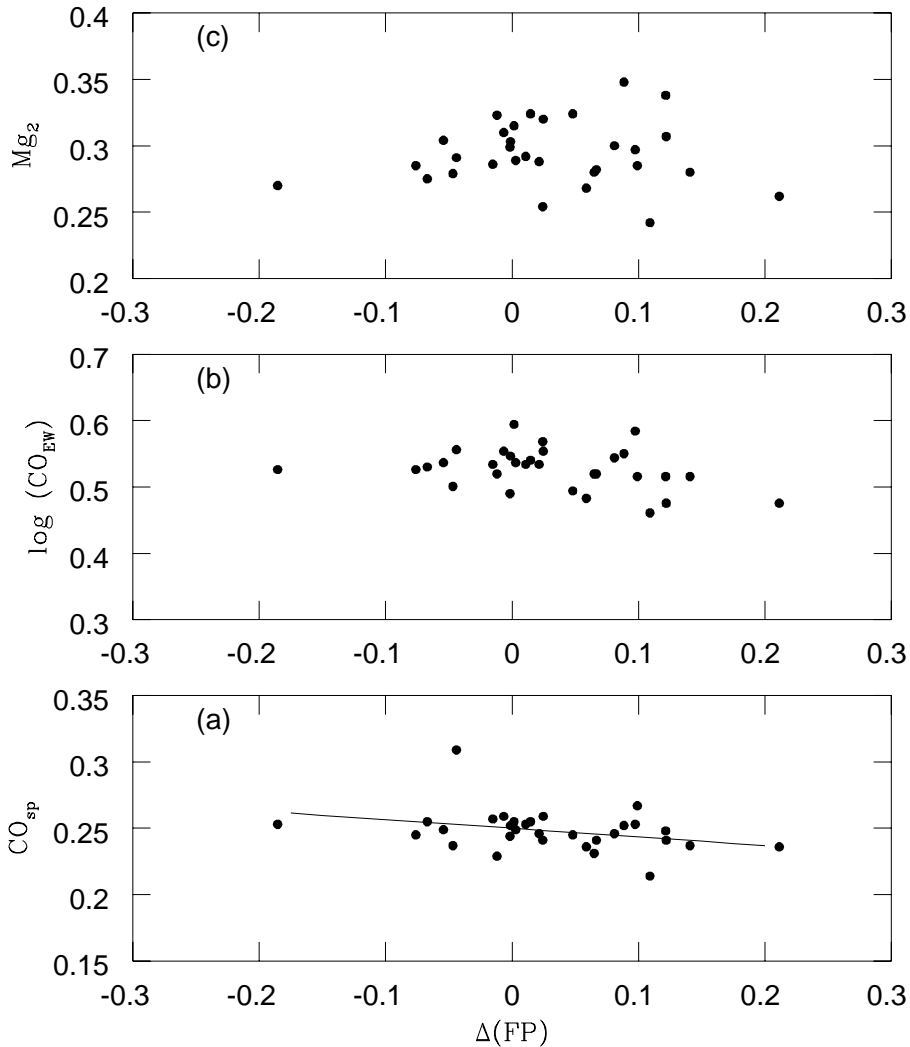


Figure 6. (a). Relation between the residuals from the near-IR FP ($\Delta(FP)$) and CO_{sp} for the Coma ellipticals; (b). the same as in Figure 6a for CO_{EW} ; (c). the same as Figure 6a for Mg_2 .

$\Delta(FP)$ *vs.* CO_{sp} relation (Figure 6a), the near-IR surface brightness of the galaxies in the present sample are corrected for contributions from the giant and supergiant populations. This reduces the *rms* scatter on the near-IR FP from 0.077 dex (Figure 5) to 0.073 dex.

Therefore, although the giant and supergiant stars make a measurable contribution to the scatter on the near-IR FP of ellipticals, their effect is rather marginal. The conclusion is that most of the observed scatter in the near-IR FP of ellipticals is either caused by observational errors or, is due to dynamical effects and non-homology among the ellipticals (Pahre et al 1998).

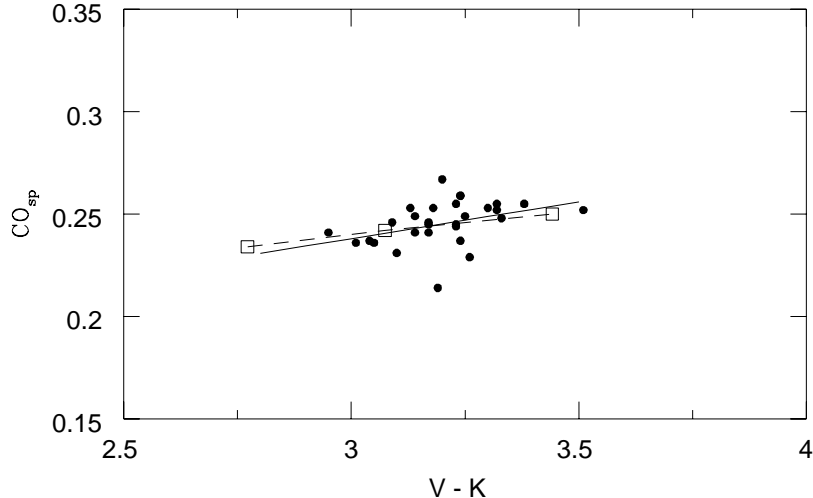


Figure 7. The $CO_{sp} - (V - K)$ relation for elliptical galaxies in the Coma cluster. Solid line is the least squares fit to the data. Predictions from stellar synthesis models of Worthey (1994), corresponding to a change in metallicity in the range $-0.5 < [Fe/H] < 0$ (increasing metallicity towards redder $V - K$ colours)- (empty boxes) is indicated. An age sequence also follows the same trend. The model is normalised to the data so that $[Fe/H] = 0$ corresponds to $V - K = 3.44$ and $CO_{sp} = 0.25$.

6 THE RELATION BETWEEN CO_{sp} AND OPTICAL-IR COLOURS OF ELLIPTICALS

The $CO_{sp} vs. V - K$ relation for 31 ellipticals in the Coma cluster (Table 1) is presented in Figure 7 with the coefficients of its best linear fit listed in Table 3. The slope of 0.036 ± 0.007 found here, is significantly shallower than 0.167 ± 0.023 , estimated for the $Mg_2 - (V - K)$ relation (derived from 47 ellipticals with available such data from Mobasher et al 1999), which represents changes in metallicity and relative contributions from young and old stellar populations among the ellipticals.

The metallicity sequence on the $CO_{sp} vs. (V - K)$ diagram, as predicted from stellar synthesis models (Worthey 1994), is also shown on Figure 7. To calculate the CO_{sp} features, not given in these models, the strength of Mg_2 lines at any given $V - K$ colours are taken from Worthey (1994) models and converted to CO_{sp} , using the empirical $Mg_2 - CO_{sp}$ relation presented in section 3. However, one should note that the main source of uncertainty here is the lack of proper modelling of the AGB and supergiant populations in these models.

The slope due to the metallicity sequence (in the range $-0.5 < [Fe/H] < 0$) in Figure 7 (dashed line), as predicted by stellar synthesis models, is close to the observed $CO_{sp} vs. (V - K)$ relation.

Table 3. Coefficients for a linear least squares fit to the $\text{CO}_{sp} - (V - K)$ relation; $Y = a * X + b$

Y	X	a	b	n
CO_{sp}	$V - K$	0.036 ± 0.016	0.130 ± 0.03	29
Mg_2	$V - K$	0.167 ± 0.023	-0.240 ± 0.061	47

K) relation (solid line in Figure 7). This is also similar to an age trend, as predicted from the same models, indicating the age/metallicity degeneracy.

Using the present data, it is not possible to determine whether age or metallicity dominate the relation shown in Figure 7, with the models showing that both are capable of producing effects of the observed size. However, the combined effect of age and metallicity appears to be significantly reduced on the $\text{CO}_{sp} - (V - K)$ diagram, as compared to that for $\text{Mg}_2 - (V - K)$ relation (Table 3).

7 CONCLUSIONS

The CO_{sp} ($2.3 \mu\text{m}$) absorption features are estimated from the near-IR spectra of a sample of 31 elliptical galaxies at the core and outskirts of the Coma cluster. Combined with other spectroscopic (σ and Mg_2) and photometric (K-band) data for this sample, a study of the stellar population in elliptical galaxies is carried out. The main conclusions from this study are summarised as follows:

- (i) The mean CO_{sp} values for elliptical galaxies at the core of the Coma cluster are found to be smaller compared to their counterparts in the outer region. There is a probability of $< 1\%$ for these galaxies belonging to the same parent population. This is interpreted as due to the presence of intermediate-age red giant and supergiant stars in ellipticals in low density environments. This implies that the ellipticals in the outskirts of rich clusters are relatively younger than their counterparts at the core.
- (ii) Using the CO_{sp} values, the near-IR FP of ellipticals is corrected for contributions from the intermediate-age supergiant stars. This reduces the *rms* scatter in this relation (at a given $\log(A_e)$) from 0.077 dex to 0.073 dex. This modest reduction means that the observed scatter on the near-IR FP of ellipticals is mostly dominated by observational errors or dynamical effects and non-homology of ellipticals.
- (iii) A relation is found between CO_{sp} and $V - K$ colours of ellipticals in the Coma cluster. The slope of this relation (0.036 ± 0.016) is significantly shallower than that for the

$Mg_2 - (V - K)$ relation. Comparing with the stellar population models, it is found that the observed trend is caused by either metallicity or stellar population changes.

REFERENCES

Aaronson, M., Cohen, J. G., Mould, J. & Malkan, M. 1978, *ApJ* 223, 824
 Abraham, R. et al 1996 *ApJ* 471, 694
 Bothun, G. & Gregg, M. 1990 *ApJ* 350, 73
 Bower R. G., Ellis R. S., Rose J. A., Sharples R. M., 1990, *AJ*, 99, 530
 Caldwell, N. et al. 1996 *AJ* 111, 78
 Doyon R., Joseph R. D., Wright G. S., 1994, *ApJ*, 421, 101
 Dressler, A., Smail, I., Poggianti, B. M., Butcher, H., Couch, W. J., Ellis, R. S. & Oemler, A. 1998, *ApJ*
 Frogel, J. A., Cohen, J. G. & Persson, S. E. 1983 *ApJ*, 275, 773
 Goldader, J.D., Joseph, R. D., Doyon, R. & Sanders, D. B. 1997 *ApJ* 474, 104
 Gonzalez, J. J. 1993 Ph.D thesis, Univ. of California, Santa Cruz
 Guzmán R., Lucey J. R., 1993, *MNRAS*, 263, 47
 James P. A. & Mobasher, B. *MNRAS* 1999, 306, 199
 Kleinmann S. G., Hall D. N. B., 1986, *ApJS*, 62, 501
 kuntschner, H. & Davies, R. 1998 *MNRAS* 295, L29
 Mobasher, B. & James, P. A., 1996, *MNRAS*, 280, 895
 Mobasher, B., Guzmán, R., Aragón- Salamanca, A. & Zepf, S. 1999 *MNRAS* 304, 225
 Pahre, M.A., Djorgovski, S.G. & de Carvalho, R.R. 1998 *ApJ* 116, 1591
 Puxley P. J., Doyon R., Ward M. J., 1997, *ApJ*, 476, 120
 Ridgway, S. E., Wynn-Williams, C. G., Becklin, E. E. 1994, *ApJ*. 428, 609
 Rose J. A., Bower R. G., Caldwell N., Ellis R. S., Sharples R. M., Teague P., 1994, *AJ*, 108, 2054
 Schweizer, F. & Seitzer, P. *AJ* 104, 1039
 Worthey, G. 1994, *ApJS*, 95, 107